

MULTIVARIATE QUANTILE-BASED PERMUTATION TESTS WITH APPLICATION TO FUNCTIONAL DATA

ZDENĚK HLÁVKA, DANIEL HLUBINKA, ŠÁRKA HUDECOVÁ

*Charles University, Faculty of Mathematics and Physics,
Department of Statistics, Prague, Czech Republic*

ABSTRACT. Permutation tests enable testing statistical hypotheses in situations when the distribution of the test statistic is complicated or not available. In some situations, the test statistic under investigation is multivariate, with the multiple testing problem being an important example. The corresponding multivariate permutation tests are then typically based on a suitable one-dimensional transformation of the vector of partial permutation p-values via so called combining functions. This paper proposes a new approach that utilizes the optimal measure transportation concept. The final single p-value is computed from the empirical center-outward distribution function of the permuted multivariate test statistics. This method avoids computation of the partial p-values and it is easy to be implemented. In addition, it allows to compute and interpret contributions of the components of the multivariate test statistic to the non-conformity score and to the rejection of the null hypothesis. Apart from this method, the measure transportation is applied also to the vector of partial p-values as an alternative to the classical combining functions. Both techniques are compared with the standard approaches using various practical examples in a Monte Carlo study. An application on a functional data set is provided as well.

1. INTRODUCTION

Permutation tests provide a powerful tool for testing statistical hypotheses in situations when the exact or asymptotic distribution of the test statistic is not readily available. Their main advantage is that they require minimal assumptions about the underlying data distribution. This is particularly useful in functional data analysis (FDA), where the data consist of functions over a continuous time domain and a parametric model would be too restrictive. Permutation tests have been successfully applied in functional regression (Cardot et al., 2007; Shi and Ogden, 2021), functional two-sample problem and ANOVA (Kashlak et al., 2023; Hlávka et al., 2022), in testing the equality of distribution functionals (Bugni and Horowitz, 2021), and in many other areas of FDA.

E-mail address: hlubinka@karlin.mff.cuni.cz.

Date: November 8, 2023.

Key words and phrases. Multivariate permutation test, multiple comparisons, optimal transport, permutation p-value decomposition.

The application of permutation tests is straightforward for a univariate test statistic, where the significance is evaluated using so called permutation distribution obtained by random permutations of the data. The corresponding p-value is computed as a proportion of permuted test statistics which are more extreme than the value computed from the original data. If the test statistic is multivariate then this approach cannot be used directly due to the lack of linear ordering in \mathbb{R}^d for $d \geq 2$, because then one cannot easily decide whether the observed value of the test statistic is extreme enough to reject the null hypothesis. Such situation arises in various practical setups, particularly within the multiple testing problem where the multiple test statistics can be seen as components of one multivariate test statistic. In that situation the Bonferroni inequality may be used to control the level of the test but it is well-known to be quite conservative, so various modifications have been proposed. A common approach is to compute so called partial p -values for each component of the vector test statistic and then combine them into a final single p-value used for the final decision about the hypothesis (Kost and McDermott, 2002; Vovk and Wang, 2020; Zhang and Wu, 2023). Within the framework of permutation tests, nonparametric combining functions allow to transform several dependent partial p -values, obtained by the univariate permutation tests applied on each component of the vector test statistic, into a single p-value, with the Liptak, Tippett, and Fisher combining functions being the most popular ones (Pesarin, 2001, Chapter 6).

In this paper, we introduce a new method for dealing with multivariate permutation tests. Namely, we propose to utilize the concept of measure transportation and the corresponding multivariate quantiles from Hallin et al. (2021) that allows to define a permutation p-value for a multivariate test statistic directly, without the need to compute the partial p-values and then combining them. The main advantages of the proposed approach are:

- it is fully distribution-free and only mild assumptions about exchangeability under the null hypothesis are required,
- there is no need to compute the partial permutation p -values and to choose a combining function since the final single permutation p -value is computed directly from the *multivariate* test statistic and its permutation counterparts,
- the approach allows to calculate and interpret contributions of the components of the vector test statistic to the rejection of the null hypothesis.

Furthermore, the method can be used for a vector test statistic even in situations when its components do not naturally correspond to some partial null hypotheses and if its components are both one-sided and two-sided.

Apart from this approach, we also consider a setup where the measure transportation is applied to the vector of the partial p-values, so the transport in some sense substitutes the combining functions. This method might be attractive to researchers who are used to working with partial p-values, or when only partial p-values are available, as, e.g., in clinical meta-analyses. However, our Monte Carlo study suggests that a transport of the original test statistic typically leads to a more powerful test.

A slightly related situation arises in the problem of synthesizing inference from multiple data sources or studies, also known as fusion learning. Recently, a depth confidence distribution combining statistical data depth function and confidence

distribution was proposed by Liu et al. (2022) as a nonparametric tool for the fusion learning that overcomes some of the shortcomings and limitations of existing methods. The notation of data depth is related to the measure transportation, but the latter one allows to interpret not only the depth of a point but also its direction from the center, which shows to be useful in the multiple testing problem.

The paper is organized as follows. In Section 2 we review multivariate tests statistics and the classical construction of scalar permutation p -values. We also provide several illustrations for the considered setup, with an emphasis on an application on functional data in Section 2.2. Section 3 describes a construction of multivariate quantiles based on the optimal measure transport to a spherically uniform distribution. The construction of permutation p -values based on this approach is discussed in Section 4. Section 5 contains a Monte Carlo study for various examples, while Section 6 illustrates the approach to functional ANOVA.

2. CLASSICAL MULTIVARIATE PERMUTATION TESTS

A permutation test is a statistical method used to assess the significance of an observed sample statistic by comparing it to a distribution of possible values obtained by permuting the observations from the sample. Consider a null hypothesis H_0 and the corresponding scalar test statistic T . Assume that the data are exchangeable under H_0 and let T_0 stand for the value of the test statistic computed from the observed data. For a chosen B repetitions, one randomly shuffles the labels of the observations and calculates the test statistics for the permuted data sets to obtain T_1, \dots, T_B . The null hypothesis is rejected whenever the observed T_0 fails to concur with T_1, \dots, T_B , and the p -value is calculated as the proportion of permuted test statistics that are more extreme than the observed test statistic.

In various situations, the test of H_0 is based on a multivariate test statistic \mathbf{T} . Then one can still use the permutation principle which now leads to multivariate permutation test statistics $\mathbf{T}_1, \dots, \mathbf{T}_B$. The classical approach is then to compute componentwise partial p -values. The resulting vector of partial p -values then needs to be combined into a single final p -value p_0 , and the value $(1 - p_0)^2$ can be interpreted as a multivariate nonconformity score because it measures, in some sense, the deviation of the data from the null hypothesis.

We illustrate this approach with a well-known toy example considering three independent random samples from shifted continuous distributions. Namely, let f be a density of an absolutely continuous distribution with a finite variance, and $X_{1,1}, \dots, X_{1,n_1}$, $X_{2,1}, \dots, X_{2,n_2}$, and $X_{3,1}, \dots, X_{3,n_3}$ be random samples with density $f(x - \mu_1)$, $f(x - \mu_2)$, and $f(x - \mu_3)$, respectively. Consider the null hypothesis

$$(1) \quad H_0 : \mu_1 = \mu_2 = \mu_3$$

against a general alternative, i.e., a three-sample problem. Note that H_0 is equivalent to the pair of hypotheses:

$$\begin{aligned} H_{0,1} : \mu_1 &= \mu_2 \\ H_{0,2} : \mu_1 &= \mu_3. \end{aligned}$$

Each hypothesis $H_{0,j}$, $j = 1, 2$, may be tested separately by a two-sample t -test. Assuming normality, the corresponding test statistics T_1 and T_2 follow t distribution under the null hypothesis. However, T_1 and T_2 are not independent and,

despite knowing their marginal distributions, their bivariate joint distribution is not tractable although the F-statistic can be used to test the null hypothesis H_0 .

The normality assumption is not needed if we rely on asymptotics or use permutation tests. Focusing on the latter approach, the partial permutation p-values can be obtained as follows:

- (P.1) Calculate the two-sample t-test statistics $T_{1,0}$ and $T_{2,0}$ from the original sample.
- (P.2) Consider a random permutation π of the set $\{1, \dots, n\}$. Let $n = n_1 + n_2 + n_3$, set $Z_1 = X_{1,1}, Z_2 = X_{1,2}, \dots, Z_n = X_{3,n_3}$, and define $X_{1,1}^* = Z_{\pi(1)}, \dots, X_{1,n_1}^* = Z_{\pi(n_1)}, X_{2,1}^* = Z_{\pi(n_1+1)}, \dots, X_{3,n_3}^* = Z_{\pi(n)}$ so that $X_{j,i}^*$ is a random permutation sample of the original (pooled) sample. Calculate the values of the test statistics T_1 and T_2 from the permuted sample.
- (P.3) Carry out B independent repetition of the step (P.2) so that the bivariate sequence $\{(T_{1,b}, T_{2,b}), b = 1, \dots, B\}$ forms a random sample from the permutation distribution of $(T_{1,0}, T_{2,0})$.
- (P.4) Compute partial p-value for the null hypothesis $H_{0,j}$ as

$$p_j = (B + 1)^{-1} \left\{ 1 + \sum_{b=1}^B \mathbf{1}(|T_{j,b}| \geq |T_{j,0}|) \right\}.$$

In this example, we have reformulated the null hypothesis H_0 in (1) in terms of two pairwise comparisons for couples (μ_1, μ_2) and (μ_1, μ_3) . In that case, the permutation procedure leads to a two-dimensional vector of p values $\mathbf{p} = (p_1, p_2)^\top$ composed of two partial p-values. An alternative approach is to consider all pairwise comparisons, which would lead, in this example, to a three-dimensional test statistic \mathbf{T} . In a general situation, one can have a d -dimensional test statistic \mathbf{T} . The permutation procedure then proceeds in an analogous way, leading to a d -dimensional vector of p-values \mathbf{p} , which needs to be combined to a single final p-value used for evaluation of the null hypothesis. This step is often based on combining functions, as described in the next section.

2.1. Combining functions. Let $\mathbf{p} = (p_1, \dots, p_d)^\top$ be a d -dimensional vector of partial p-values obtained by a permutation procedure performed on the components of \mathbf{T} . Let $f : [0, 1]^d \rightarrow [0, 1]$ be a selected combining function. The multivariate permutation test of H_0 based on a combining function f proceeds in the following way:

- (C.1) For $b = 1 \dots, B$ and $j = 1, \dots, d$ define

$$p_{j,b} = (B + 1)^{-1} \left\{ 1 + \sum_{s=1}^B \mathbf{1}(|T_{j,s}| \geq |T_{j,b}|) \right\}.$$

a permutation p-value which would correspond to the test statistic $T_{j,b}$.

Let $\mathbf{p}_b = (p_{1,b}, \dots, p_{d,b})^\top$.

- (C.2) Define $Q_0 = f(\mathbf{p})$ and $Q_b = f(\mathbf{p}_b)$, for $b = 1, \dots, B$.
- (C.3) The multivariate permutation p-value is then defined as

$$p_0 = (B + 1)^{-1} \left\{ 1 + \sum_{b=1}^B \mathbf{1}(Q_b \geq Q_0) \right\}.$$

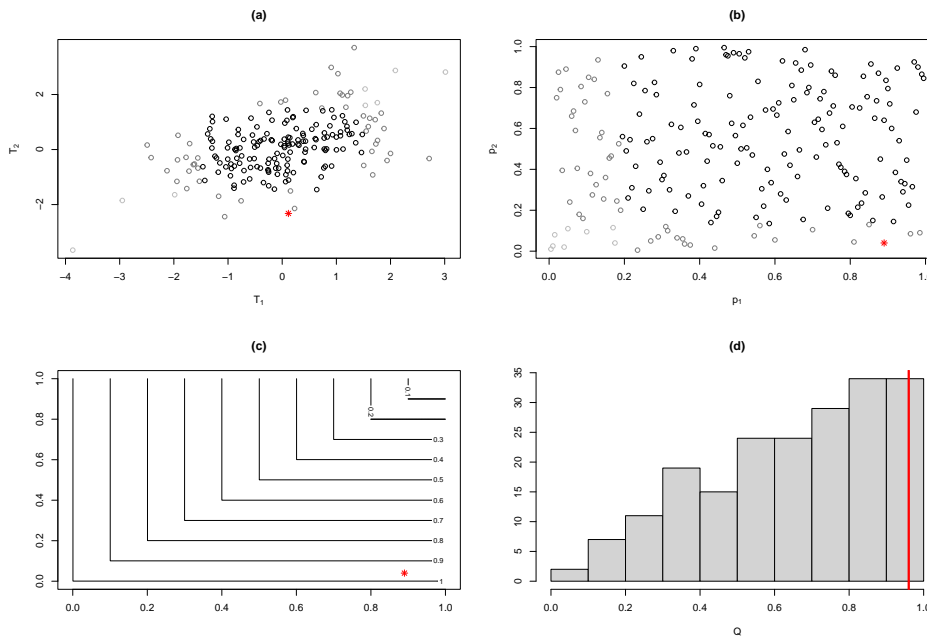


FIGURE 1. Bivariate permutation test with Tippett combining function: (a) bivariate permutation test statistics $(T_{1,b}, T_{2,b})$, red star denotes (T_1, T_2) , $B = 199$, (b) partial permutation p-values $(p_{1,b}, p_{2,b})$, red star denotes the observed (p_1, p_2) , (c) Tippett combining function $f_T(\cdot, \cdot)$, (d) histogram of Q_b , vertical red line denotes Q_0 , multivariate permutation p-value $p_0 = 0.065$.

Commonly used combining functions are the Tippett combining function $f_T(\mathbf{p}) = \max_{1 \leq j \leq d} (1 - p_j)$, the Liptak combining function $f_L(\mathbf{p}) = \sum_{j=1}^d \Phi^{-1}(1 - p_j)$, and the Fisher omnibus combining function $f_F(\mathbf{p}) = -2 \sum_{j=1}^d \log(p_j)$.

A simulated example using the Tippett combining function with $n_1 = n_2 = n_3 = 8$, $\mu_1 = \mu_2 = 1$, and $\mu_3 = 2$ with $\sigma = 1$ is plotted in Figure 1. Following the multivariate permutation test algorithm, with each step illustrated in Figure 1, we arrive to the multivariate permutation p-value $p_0 = 0.065$ and we do not reject the null hypothesis H_0 on confidence level $\alpha = 0.05$. This result strongly depends on the choice of the combining function and different p-values could be obtained simply by using another combining function. In our simulated example, p-values 0.140 and 0.360 are obtained, respectively, by applying the Fisher and Liptak combining function.

Remark. Another possibility for obtaining a final single p-value is via a suitable scalar function of $\mathbf{T}_0, \mathbf{T}_1, \dots, \mathbf{T}_B$, for example, their l_p norm for some $p \in [1, \infty]$. This approach is called a *direct combination* but it is recommended only for test statistics with the same marginal asymptotic distributions and for a large sample size, see Pesarin (2001, Section 6.2.4 (h)).

2.2. More general setups. The simple three samples problem from the beginning of this section serves mainly for an illustration of the multivariate permutation testing approach, but the problem of multiple testing occurs, of course, in many more complex situations.

2.2.1. Testing equality of r moments. A multivariate test statistic naturally arises when one wants to test equality of moments up to a prescribed order $r \geq 2$ for $K \geq 2$ samples. Assume that $X_{j,1}, \dots, X_{j,n_j}$ are independent random variables from a distribution F_j with $\int_{-\infty}^{\infty} |x|^r dF_j(x) < \infty$ for $j = 1, \dots, K$ and these K samples are independent. Denote as $\mu_s^{(j)} = \int_{-\infty}^{\infty} x^s dF_j(x) < \infty$, $s = 1, \dots, r$ the non-central moment for j -th sample. Consider the joint null hypothesis

$$H_0 : \mu_s^{(1)} = \dots = \mu_s^{(K)} \quad \text{for all } s = 1, \dots, r,$$

which can be decomposed into r marginal hypotheses $H_{0,s} : \mu_s^{(1)} = \dots = \mu_s^{(K)}$ for $s = 1, \dots, r$. Each of them can be tested in terms of a suitable version of ANOVA applied on $X_{i,j}^s$, or alternatively further decomposed to pairwise comparisons, leading generally to a d dimensional test statistic \mathbf{T} . If the data are exchangeable under the null hypothesis H_0 , then the permutation principals may be used for \mathbf{T} .

2.2.2. Functional data. There are many real-world situations where the system is observed over a continuous time domain, such as economics, meteorology, medicine, and more. Functional Data Analysis (FDA) is an active area of statistics, which deals with data in the form of functions. Permutation techniques, analogous to those described in Section 2.1, serve as a standard tool in FDA testing, because the (asymptotic) distribution of a considered test statistic is typically very complex even under the null hypothesis.

In what follows we assume that a functional random variable X is a random element in a Banach space $\mathcal{X} = \mathcal{L}_2[0, 1]$ of square integrable functions on $[0, 1]$. The space \mathcal{X} is equipped with an inner product $\langle u, v \rangle = \int_0^1 u(t)v(t)dt$, $u, v \in \mathcal{X}$, and induced norm $\|u\| = \sqrt{\langle u, u \rangle}$. Namely, if $(\Omega, \mathcal{A}, \mathbb{P})$ is a probability space, then we say that $X : \Omega \rightarrow \mathcal{X}$ is a functional random variable if the real-valued random variable $\|X\| : \Omega \rightarrow \mathbb{R}$ has finite second moment, i.e., if $\mathbb{E} \int_0^1 X^2(t)dt < \infty$. A distribution of a functional random variable X can be described by a characteristic function, which is defined as

$$\phi(w) = \mathbb{E} e^{i\langle w, X \rangle}, \quad w \in \mathcal{X}.$$

Other useful characteristics are the mean function $\mu(t) = \mathbb{E}X(t)$ and the covariance operator $C : \mathcal{X} \rightarrow \mathcal{X}$ defined as $C(y) = \mathbb{E}\langle X - \mu, y \rangle(X - \mu)$, $y \in \mathcal{X}$.

Consider a functional K -sample problem. Let $X_{j,1}, \dots, X_{j,n_j}$ be independent and identically distributed functional observations with a characteristic function ϕ_j , mean μ_j and covariance operator C_j for $i = 1, \dots, n_j$, $j = 1, \dots, K$, and let the K samples be independent. A general null hypothesis of equality of the whole distributions is stated as

$$H_0 : \phi_1 = \dots = \phi_K.$$

For the two sample problem, $K = 2$, Hlávka et al. (2022) propose a test statistic T_{12} for testing H_0 based on empirical analogues of the characteristic functions ϕ_j , $j = 1, 2$. The null hypothesis is rejected for large values of T_{12} (one-sided test). The significance of T_{12} is evaluated via a permutation test, which can be applied here, because all the observations are exchangeable under H_0 , and which is a complete

analogy to the procedure described in Section 2.1. For $K > 2$, the null hypothesis H_0 can be reformulated in terms of all $\binom{K}{2}$ pairwise comparisons $H_{0,kl} : \phi_k = \phi_l$ for all $1 \leq k < l \leq K$. Each $H_{0,kl}$ can be tested using the permutation two-sample test statistic $T_{k,l}$, leading to a $d = \binom{K}{2}$ dimensional vector of all test statistics \mathbf{T} and d dimensional vector of partial permutation p-values \mathbf{p} .

Alternatively, one may focus on the equality of the mean functions in terms of the null hypothesis

$$H_0^M : \mu_1 = \cdots = \mu_K,$$

or equality of covariance operators

$$H_0^C : C_1 = \cdots = C_K.$$

Various tests have been proposed for testing the hypothesis H_0^M or H_0^C for a general K sample problem (Zhang, 2013; Cuevas et al., 2004; Górecki and Smaga, 2015; Cuesta-Albertos and Febrero-Bande, 2010; Górecki and Smaga, 2019). However, one may want to test these two hypothesis jointly, i.e. to consider $H_0^{CM} : \mu_1 = \cdots = \mu_K$ & $C_1 = \cdots = C_K$. If the data are exchangeable under the null hypothesis H_0^{CM} , then one can use permutation tests for testing H_0^M and H_0^C separately, leading to a two-dimensional test statistic \mathbf{T} and a vector of partial permutation p-values \mathbf{p} . This approach is illustrated on a real data set in Section 6.

2.3. Two-sided vs one-sided test statistics. In the following we will sometimes need to distinguish whether the test statistic \mathbf{T} under investigation is two-sided, one-sided or a combination of both. The meaning of these terms is explained in the next paragraphs.

The multivariate permutation test from Section 2.1 is based on a two-dimensional test statistic $\mathbf{T} = (T_1, T_2)^\top$, whose components correspond to the null hypotheses $H_{0,j}$, $j = 1, 2$. Each of the two partial tests is two-sided in a sense that the null hypothesis $H_{0,j}$ is rejected for large values of $|T_j|$. However, there are various statistical tests which are one-sided, so the null hypothesis is rejected only when the corresponding univariate test statistic is larger than a given critical value while it is not rejected for small values (e.g. χ^2 test, F test, one sided t -test etc.). A similar situation can occur also with a multivariate test statistic. For instance in some specific regression problems one may want to test the joint significance of the vector of regression parameters against an alternative that all the effects are positive, i.e. to test $H_0 : \boldsymbol{\beta} = \mathbf{0}$ against $H_1 : \boldsymbol{\beta} > \mathbf{0}$, where the inequality is taken componentwise. Then the least squares estimator $\hat{\boldsymbol{\beta}}$ can be considered as a multivariate test statistic and the corresponding testing problem is one-sided. Some other examples of one-sided multivariate tests are presented in Section 2.2.2.

Finally, some practical situations can lead to a multivariate test statistic \mathbf{T} composed by two-sided and one-sided test statistics. For instance, in a two-sample setup, one may want to test the joint hypothesis of equality of means and variance while considering a two-sided alternative for the means and one-sided alternative for the variances.

3. MULTIVARIATE QUANTILES BASED ON MEASURE TRANSPORTATION

There exist several approaches intending to define multivariate ranks and quantiles, often based on some depth function, directions, or optimal ellipsoids; see, e.g., Chaudhuri (1996); Pokorný et al. (2023); Chandler and Polonik (2022); Hlubinka et al. (2022); Hlubinka and Šiman (2015); Koshevoy and Mosler (1998). Recently,

results from the optimal measure transportation (Villani, 2021; Figalli and Glaudo, 2021) have been successfully applied in this context, resulting in the so called center-outward (CO) distribution function and quantiles (Chernozhukov et al., 2017; Hallin et al., 2021). The corresponding ranks and signs have been applied in various multivariate statistical problems, see, e.g., Shi et al. (2022); Hallin et al. (2023, 2022). In what follows we utilize this technique since it offers possibility to construct also multivariate versions of “one-sided” tests.

Let U_d denote a distribution on the unit ball $\mathbb{S}_d = \{\mathbf{x} \in \mathbb{R}^d; \|\mathbf{x}\| \leq 1\}$ corresponding to a random variable $U\mathbf{S}$, where U is uniformly distributed on $[0, 1]$ and it is independent of \mathbf{S} , which has a uniform distribution on the unit sphere $\mathcal{S}_{d-1} = \{\mathbf{x} \in \mathbb{R}^d; \|\mathbf{x}\| = 1\}$.

Let P be an absolute continuous distribution on \mathbb{R}^d . McCann (1995) proved that there exists a convex map ψ_P such that its gradient $\nabla\psi_P$ pushes P to U_d , i.e., if a random vector $\mathbf{Z} \sim P$, the random vector $\nabla\psi_P(\mathbf{Z}) \sim U_d$. Moreover, the gradient $\nabla\psi_P$ is P -a.s. unique. If the distribution P has finite second moments, the transformation $\nabla\psi_P$ is optimal with respect to the quadratic loss function, i.e., $\mathbb{E}\|\mathbf{Z} - \nabla\psi_P(\mathbf{Z})\|^2 = \min_{\mathbf{Y} \sim U_d} \mathbb{E}\|\mathbf{Z} - \mathbf{Y}\|^2$, see Figalli and Glaudo (2021, Chapter 2). The mapping $\nabla\psi_P$ is called the *center-outward distribution function* and it is denoted as F_{\pm} , see Hallin et al. (2021). Since $F_{\pm}(\mathbf{Z}) \sim U_d$ is spherically symmetric, and $\|F_{\pm}(\mathbf{Z})\|$ is uniformly distributed on $[0, 1]$, it is natural to define the α -quantile contour of P as the set $\mathcal{T}_{P,\alpha} = \{\mathbf{x}; \|F_{\pm}(\mathbf{x})\| = \alpha\}$, and the α -quantile region of P as $\mathbb{T}_{P,\alpha} = \{\mathbf{x}; \|F_{\pm}(\mathbf{x})\| \leq \alpha\}$.

Consider a random sample $\mathbf{Z}_1, \dots, \mathbf{Z}_n$ from the distribution P . The empirical counterpart $F_{\pm}^{(n)}$ of F_{\pm} is defined as the mapping from $\mathbf{Z}_1, \dots, \mathbf{Z}_n$ to a given regular grid \mathcal{G}_n of n points in the unit ball \mathbb{S}_d such that the mapping minimizes the sum of squared Euclidean distances $\sum_{i=1}^n \|F_{\pm}^{(n)}(\mathbf{Z}_i) - \mathbf{Z}_i\|^2$. A Glivenko-Cantelli result holds for $F_{\pm}^{(n)}$ and F_{\pm} whenever $F_{\pm}^{(n)}$ is computed on a sequence of grids $\{\mathcal{G}_n\}$ such that the discrete uniform distribution on \mathcal{G}_n converges weakly to U_d .

Using $F_{\pm}^{(n)}$ the empirical α -quantile region can be defined as a collection of observed points

$$\{\mathbf{Z}_i : \|F_{\pm}^{(n)}(\mathbf{Z}_i)\| \leq \alpha\}.$$

The problem of turning such set into continuous contours enclosing compact regions is studied in Hallin et al. (2021, Section 3).

3.1. Transportation grid. The computation of the sample CO distribution function requires a choice of the target grid \mathcal{G}_n . Hallin et al. (2021) recommends to use a product form grid, but some other types of grids also proved to be useful in the statistical testing, see, e.g., Hallin and Mordant (2023) or Hlubinka and Hudecova (2023).

The construction of a grid \mathcal{G}_n in \mathbb{S}_d , $d \geq 2$, often makes use of so called low-discrepancy points from $[0, 1]^r$ for $r = d$ or $r = d - 1$. Recall that a low-discrepancy sequence $\{\mathbf{x}_k\}_{k=1}^K$ of K points in $[0, 1]^r$ is a deterministic sequence designed to be “as uniform as possible” in a sense that it minimizes the discrepancy between the distribution of $\{\mathbf{x}_k\}_{k=1}^K$ and a uniform distribution in $[0, 1]^r$, see (Fang and Wang, 1994, Section 1.2). Roughly speaking, the proportion of points from $\{\mathbf{x}_k\}_{k=1}^K$ falling into any rectangle $A \subset [0, 1]^r$ should be close to the volume of A . There are various approaches to the construction of such sequences, the most popular ones are Halton

sequences (Halton, 1960), Sobol sequences (Sobol, 1967), or good-lattice-point sets (GLP) (Fang and Wang, 1994, Section 1.3).

In this paper, we consider the following two types of grids:

- A product form grid (abbreviated as \mathcal{P}) as a union of n_0 replicas of $\mathbf{0}$ and points

$$\mathbf{g}_{ij} = \frac{i}{n_R + 1} \mathbf{s}_j, \quad i = 1, \dots, n_R, \quad j = 1, \dots, n_S,$$

for $n = n_R \cdot n_S + n_0$, where \mathbf{s}_j are unit vectors from the unit sphere \mathcal{S}_{d-1} obtained as a suitable transformation (see below) of low-discrepancy points in $[0, 1]^{d-1}$. Moreover, n_0 is negligible compared to n_R and n_S , typically $n_0 \in \{0, 1\}$.

- A non-product form grid (abbreviated as \mathcal{N}) $\mathcal{G}_n = \{\mathbf{g}_i\}_{i=1}^n$ obtained from a low-discrepancy sequence of points $\mathbf{x}_1, \dots, \mathbf{x}_n$ in $[0, 1]^d$ such that

$$\mathbf{g}_i = x_{i,1} \cdot \mathbf{s}_i, \quad i = 1, \dots, n,$$

where $\mathbf{x}_i = (x_{i,1}, \dots, x_{i,d})^\top$ and the vector $(x_{i,2}, \dots, x_{i,d})^\top \in [0, 1]^{d-1}$ is transformed to a vector $\mathbf{s}_i \in \mathcal{S}_{d-1}$ using a suitable transformation (see below).

The transformation $\tau : [0, 1]^{d-1} \rightarrow \mathcal{S}_{d-1}$ of points from $[0, 1]^{d-1}$ to the vectors from the unit sphere has to be such that if a random vector \mathbf{X} has a uniform distribution on $[0, 1]^{d-1}$ then $\mathbf{S} = \tau(\mathbf{X})$ has a uniform distribution on \mathcal{S}_{d-1} . Such τ is described in Fang and Wang (1994, Section 1.5.3) for general $d \geq 2$. Particularly, if $d = 2$ then the corresponding transformation $\tau : [0, 1] \rightarrow \mathcal{S}_1$ is simply

$$\tau(x) = (\cos(2\pi x), \sin(2\pi x))^\top.$$

In addition, for $d = 2$ the sequence of K points $\{(2k-1)/(2K)\}_{k=1}^K$ has the lowest possible discrepancy, so the directions \mathbf{s}_j of the grid \mathcal{P} can be chosen completely regularly for any n_S using this sequence and the transformation τ . For $d = 3$ the suitable transformation $\tau : [0, 1]^2 \rightarrow \mathcal{S}_2$ is

$$\tau(\mathbf{x}) = \left(1 - 2x_1, 2\sqrt{x_1(1-x_1)} \cos(2\pi x_2), 2\sqrt{x_1(1-x_1)} \sin(2\pi x_2) \right)^\top$$

for $\mathbf{x} = (x_1, x_2)^\top$.

An example of the two types of grids for $n = 144$ in $d = 2$ is shown in Figure 2. The product type grid (left panel) is constructed as described in the previous paragraph with $n_R = n_S = 12$. The non-product grid (right panel) uses a GLP sequence in $[0, 1]^2$ generated by vector $(1, 89)^\top$. Figure 3 provides an example of the two types of grids in $d = 3$. Namely, the product type grid (left panel) is formed by $n = 1100$ points with $n_S = 55$ and $n_R = 20$, where the unit vectors \mathbf{s}_j were computed from a GLP sequence in $[0, 1]^2$ (generating vector $(1, 34)^\top$). A non-product grid was obtained as a transformation of $n = 1010$ GLP points in $[0, 1]^3$ (generating vector $(1, 140, 237)^\top$). Some practical aspects related to the choice and computation of the target grids are described in more detail in Section 4.3. We also provide an online example on web page https://www.karlin.mff.cuni.cz/~hudecova/research/mult_perm/Main.html for both $d = 2$ and $d = 3$. For $d = 3$ the the two types of grids are plotted therein using 3D interactive plots which enable one to rotate them and explore them in more detail.

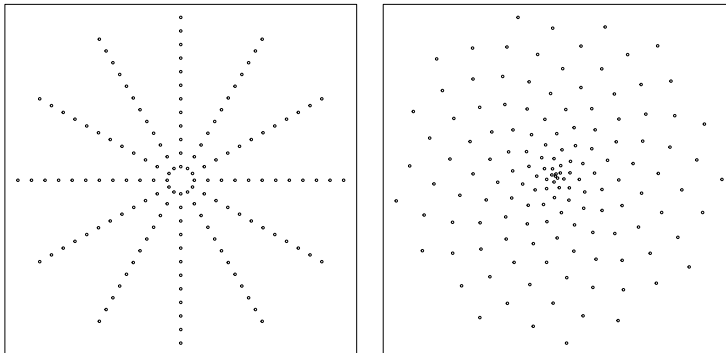


FIGURE 2. Two different grids of $n = 144$ points in \mathbb{S}_2 : product-form grid \mathcal{P} with $n_R = n_S = 12$ and $n_0 = 0$ (left panel) and a non-product grid \mathcal{N} based on a GLP set generated by the vector $(1, 89)^\top$ (right panel).

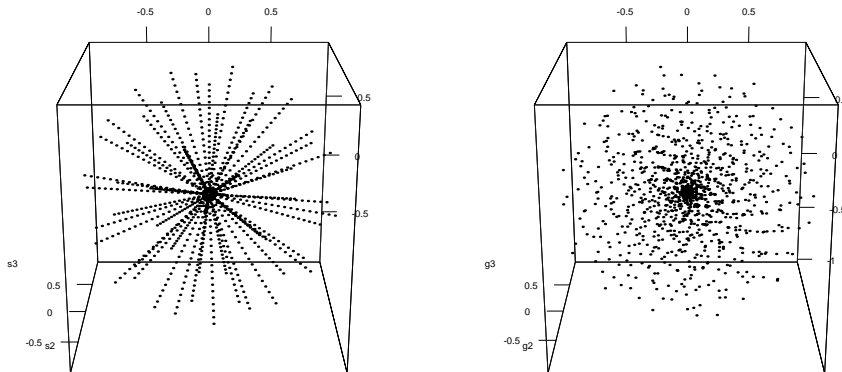


FIGURE 3. A product type grid \mathcal{P} (left panel) and a non-product type grid \mathcal{N} (right panel) for $d = 3$.

3.2. Modifications. The CO distribution function F_\pm corresponds to the transformation of P to the spherically uniform distribution U_d . Instead of U_d some authors consider a different reference measure μ , see Chernozhukov et al. (2017) or Ghosal and Sen (2022). The corresponding mapping \tilde{F} then pushes P to μ , and the empirical counterpart of \tilde{F} naturally requires a different grid \mathcal{G}_n . For instance, if μ is uniform on $[0, 1]^d$ then \mathcal{G}_n should be a set of n points “as uniform as possible” in $[0, 1]^d$.

In Section 4.2 we consider a grid \mathcal{G}_n^+ which corresponds to μ being a restriction of U_d on $[0, 1]^d$, i.e. a distribution of a random vector $U \cdot \tilde{\mathbf{S}}$, where U is uniformly distributed on $[0, 1]$ independent of $\tilde{\mathbf{S}}$ which is uniformly distributed on $\{\mathbf{x} \in [0, 1]^d : \|\mathbf{x}\| = 1\}$. The grid \mathcal{G}_n^+ can be again chosen in a product form or non-product form, see Section 4.2 for more details.

4. APPLICATION TO PERMUTATION TESTS

Let H_0 be a null hypothesis which can be tested using a permutation test based on a test statistic \mathbf{T} . Let \mathbf{T}_0 stand for the value of the test statistic computed from the original data, and let $\mathbf{T}_1, \dots, \mathbf{T}_B$ be the permutation counterparts obtained by a permutation principal analogous to the one described in Section 2.

In what follows we assume that the distribution of the data as well as the distribution of the test statistic \mathbf{T} is absolutely continuous, and that the test of interest is two-sided. The latter assumption is removed in Section 4.4.

4.1. Transportation of the multivariate test statistics. Rather than combining the d univariate p-values corresponding to the coordinates of \mathbf{T} , we utilize the center outward approach.

Let \mathcal{G}_B be a grid of $B + 1$ points $\mathbf{g}_i, i = 0, \dots, B$, from the unit ball \mathbb{S}_d and let $F_{\pm}^{(B)}$ be the empirical CO distribution function which maps $\mathbf{T}_0, \mathbf{T}_1, \dots, \mathbf{T}_B$ to \mathcal{G} . An example of such mapping $F_{\pm}^{(B)}$ in $d = 2$ and a regular product-form grid \mathcal{G} is shown in Figure 4.

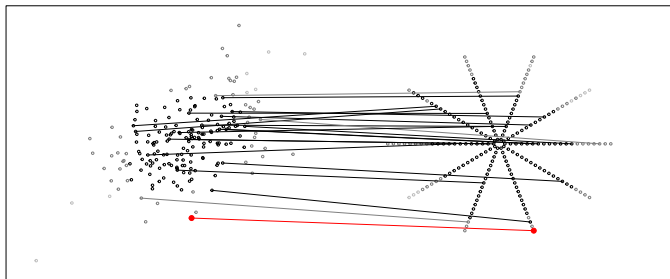


FIGURE 4. The optimal CO transport $F_{\pm}^{(B)}$ of the observed bivariate test statistic \mathbf{T}_0 (large red point) and the corresponding permutation random variables $\mathbf{T}_1, \dots, \mathbf{T}_B, B = 199$.

The (standard) bivariate permutation p-value is estimated as the relative frequency

$$(2) \quad \hat{p}_e = \frac{1}{B+1} \left(1 + \sum_{b=1}^B \mathbf{1}(\|F_{\pm}^{(B)}(\mathbf{T}_b)\| \geq \|F_{\pm}^{(B)}(\mathbf{T}_0)\|) \right),$$

i.e., the relative proportion of points \mathbf{g}_i that are more distant from the center than the point $F_{\pm}^{(B)}(\mathbf{T}_0)$.

Alternatively, the p-value can be approximated also as

$$(3) \quad \hat{p}_a = 1 - \|F_{\pm}^{(B)}(\mathbf{T}_0)\|,$$

i.e. the distance of the transported (bivariate) test statistic to the unit circle.

The whole procedure is summarized in Algorithm 1. Some practical aspects of the particular steps 1.–5. are discussed in more detail in Section 4.5.

Algorithm 1 Transportation of multivariate test statistics

Input: A d -variate two-sided test statistic \mathbf{T}_0 for testing H_0 .

- 1: Choose the number of permutations B .
- 2: Compute grid \mathcal{G}_B of $B + 1$ points.
- 3: Compute permutation test statistics $\mathbf{T}_1, \dots, \mathbf{T}_B$.
- 4: Compute the transport $F_{\pm}^{(B)}$.
- 5: Calculate the p-value as \hat{p}_e or \hat{p}_a .

Output: A scalar p-value of significance of H_0

Remark. Consider a product type grid $\mathcal{G}_B = \mathcal{P}_B$ with $B + 1 = n_R n_S + n_0$. If n_R is large then the difference between \hat{p}_e and \hat{p}_a is negligible, and both \hat{p}_e and \hat{p}_a follow under the null hypothesis a distribution that is approximately the uniform distribution over $[0, 1]$.

Indeed, \hat{p}_e in (2) takes values in $\left\{\frac{k}{n_R n_S + n_0}, k = n_S, 2n_S, \dots, n_R n_S\right\} \cup \{1\}$. Under the null hypothesis the values in the first set are attained with equal probabilities $\frac{n_S}{n_R n_S + n_0}$, and $\hat{p}_e = 1$ with probability $\frac{n_0}{n_R n_S + n_0}$. Further, \hat{p}_a in (3) attains values from $\left\{\frac{k}{n_R + 1}, k = 1, \dots, n_R\right\} \cup \{1\}$, where all values in the first set are attained with the same probability $\frac{n_S}{n_R n_S + n_0}$ and $\hat{p}_a = 1$ with probability $\frac{n_0}{n_R n_S + n_0}$. Since n_0 is always chosen negligible compared to n_R and n_S , we get the desired distributional properties of \hat{p}_e and \hat{p}_a .

In addition, if $n_0 = 0$ then the sets of possible values of \hat{p}_e and \hat{p}_a are $\left\{\frac{k}{n_R}, k = 1, \dots, n_R\right\}$ and $\left\{\frac{k}{n_R + 1}, k = 1, \dots, n_R\right\}$, respectively, and it holds that

$$\hat{p}_a = \hat{p}_e \frac{n_R}{n_R + 1},$$

which shows that their difference is negligible for a large n_R .

Remark (Handling the ties). Although we assume that \mathbf{T} has an absolutely continuous distribution, we cannot completely exclude the occurrence of ties among $\mathbf{T}_1, \dots, \mathbf{T}_B$. For instance for the three sample problem from Section 2, there are at most $\frac{n!}{n_1! n_2! n_3!}$ different results of the permuted statistics and we make B permutations, therefore, there is a non-zero probability that $\mathbf{T}_i = \mathbf{T}_j$ for $i \neq j$. In such a case a randomization approach needs to be used when computing $F_{\pm}^{(B)}$. However, the probability of such event is quite small and our practical experiments indicate that the occurrence of ties can be neglected in practice.

4.2. Transportation of the partial permutation p-values. The approach from the previous section allows us to order the multivariate variables $\mathbf{T}_0, \mathbf{T}_1, \dots, \mathbf{T}_B$ and to compute corresponding empirical quantiles, and the computation of the partial permutation p-values is not required. This section describes an alternative method.

Let $\mathbf{p} = (p_1, \dots, p_d)^\top$ be the vector of partial permutation p-values computed from \mathbf{T}_0 and let $\mathbf{p}_b = (p_{1,b}, \dots, p_{d,b})$ be the vector of partial p-value corresponding to the components of \mathbf{T}_b , $b = 1, \dots, B$, as described in Section 2.1. Recall that the classical multivariate permutation test uses a combining function f to transform the vector \mathbf{p}_b to a scalar statistic Q_b . Instead of this, we propose to apply the measure transportation techniques on \mathbf{p}_b . In order to stay consistent with the concept of “rejecting for large values”, we do not transport the partial p-values directly, but

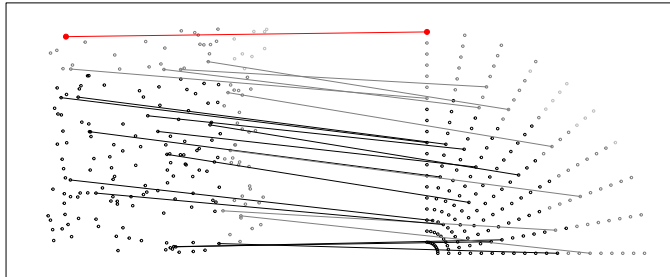


FIGURE 5. Transport of complements \mathbf{q}_b , $b = 1, \dots, B$, of vectors of partial permutation p-values onto a product grid \mathcal{P}_B^+ of $B + 1 = 200$ points.

via their complements. Define

$$\mathbf{q}_0 = (1 - p_1, \dots, 1 - p_d)^\top, \quad \mathbf{q}_b = (1 - p_{1,b}, \dots, 1 - p_{d,b})^\top.$$

Then the j th partial test statistic is significant if and only if j th component of \mathbf{q}_0 is larger than the significance level. Hence, the components of \mathbf{q}_0 behave similarly as test statistics of one sided tests, so it is not suitable to transport the points \mathbf{q}_b , $b = 0, \dots, B$ to the same grid as in Section 4.1. Instead, we will make use of a regular grid \mathcal{G}_B^+ of $B + 1$ points in the set $\{\mathbf{x} \in [0, 1]^d : \|\mathbf{x}\| \leq 1\}$. Namely, we use two types of grids analogous to those from Section 3.1:

- a product form grid, abbreviated as \mathcal{P}^+ , which consists of points $\mathbf{g}_{ij} = \frac{i}{n_R+1} \mathbf{s}_j$ for $i = 1, \dots, n_R$, and $j = 1, \dots, n_S$, $B + 1 = n_R n_S$, where \mathbf{s}_j are computed as a suitable transformation of a low-discrepancy sequence in $[0, 1]^{d-1}$ to the set $\{\mathbf{x} \in [0, 1]^d : \|\mathbf{x}\| = 1\}$,
- a non-product form grid, denoted as \mathcal{N}^+ , consisting of directly transformed $B + 1$ low-discrepancy points in $[0, 1]^d$ to the set $\{\mathbf{x} \in [0, 1]^d : \|\mathbf{x}\| \leq 1\}$.

Analogously as in Section 3, one calculates $\tilde{F}_\pm^{(B)}$ as a mapping of $\mathbf{q}_0, \mathbf{q}_1, \dots, \mathbf{q}_B$ to \mathcal{G}_B^+ , which minimizes the squared Euclidean distances. The resulting p-value of the permutation test of H_0 can be then computed as

$$\tilde{p}_e = \frac{1}{1 + B} \sum_{b=1}^B \mathbf{1} \left(\|\tilde{F}_\pm^{(B)}(\mathbf{q}_b)\| \geq \|\tilde{F}_\pm^{(B)}(\mathbf{q}_0)\| \right),$$

or simply as $\tilde{p}_a = 1 - \|\tilde{F}_\pm^{(B)}(\mathbf{q}_0)\|$.

An example of a transport $\tilde{F}_\pm^{(B)}$ of \mathbf{q}_b , $b = 0, \dots, B$, obtained in the simulated example in Section 2.1 to a product form grid is plotted in Figure 5 for $B + 1 = 200$. The whole procedure is summarized in Algorithm 2, while some practical aspects on the particular steps are postponed to Section 4.5.

4.3. Interpretation of partial contributions. Unlike the multivariate permutation tests, the optimal transport approach provides also additional information

Algorithm 2 Transportation of multivariate permutation p-values**Input:** A d -variate test statistic \mathbf{T}_0 for testing H_0 .

- 1: Choose the number of permutations B .
- 2: Compute grid \mathcal{G}_B^+ of $B + 1$ points.
- 3: Compute permutation test statistics $\mathbf{T}_1, \dots, \mathbf{T}_B$.
- 4: Compute the partial permutation p-values and the corresponding vectors of complements \mathbf{q}_j , $j = 0, 1, \dots, B$.
- 5: Compute the transport $\tilde{F}_\pm^{(B)}$.
- 6: Calculate the p-value as \tilde{p}_e or \tilde{p}_a .

Output: A scalar p-value of significance of H_0

on the importance of the marginal hypotheses. Consider first the approach from Section 4.1, where the test statistics $\mathbf{T}_0, \dots, \mathbf{T}_B$ are transported via mapping $F_\pm^{(B)}$.

Apart from the p-value computed from $F_\pm^{(B)}(\mathbf{T}_0)$, the direction vector

$$\mathbf{D} = (D_1, \dots, D_d)^\top = \frac{F_\pm^{(B)}(\mathbf{T}_0)}{\|F_\pm^{(B)}(\mathbf{T}_0)\|}$$

can reveal how the partial statistics $T_{j,0}$, $j = 1, \dots, d$, contribute to the rejection of H_0 . As mentioned in Section 2, $(1 - \hat{p}_a)^2$ can be interpreted as a non-conformity score which measures the deviation from the null hypothesis. It follows from (3) that $\|F_\pm^{(B)}(\mathbf{T}_0)\|^2 = (1 - \hat{p}_a)^2$, so we obtain a decomposition

$$(1 - \hat{p}_a)^2 = \|F_\pm^{(B)}(\mathbf{T}_0)\|^2 = \sum_{j=1}^d F_{\pm,j}^{(B)}(\mathbf{T}_0)^2,$$

where $F_\pm^{(B)}(\mathbf{T}_0) = \left(F_{\pm,1}^{(B)}(\mathbf{T}_0), \dots, F_{\pm,d}^{(B)}(\mathbf{T}_0)\right)^\top$. Hence, $F_{\pm,j}^{(B)}(\mathbf{T}_0)^2$ can be interpreted as an absolute contribution of the j -th partial test statistic to the rejection of the composite null hypothesis because the null hypothesis is not rejected if the sum of these contributions is too small. When the null hypothesis is rejected, it makes sense to consider

$$(4) \quad (D_1^2, \dots, D_d^2) = \frac{\left(F_{\pm,1}^{(B)}(\mathbf{T}_0)^2, \dots, F_{\pm,d}^{(B)}(\mathbf{T}_0)^2\right)}{\|F_\pm^{(B)}(\mathbf{T}_0)\|^2}$$

that can be interpreted as a relative contribution of the j -th partial test statistic in terms of percentages because $\sum_i D_i^2 = 1$.

Similarly, if the method from Section 4.2 is used and the partial permutation p-values are transported via $\tilde{F}_\pm^{(B)}$, then one can define the vector of individual contributions as

$$\frac{\left(\tilde{F}_{\pm,1}^{(B)}(\mathbf{q}_0)^2, \dots, \tilde{F}_{\pm,d}^{(B)}(\mathbf{q}_0)^2\right)}{\|\tilde{F}_\pm^{(B)}(\mathbf{q}_0)\|^2}.$$

We illustrate this concept on the three sample example from Section 2, where $H_{0,1} : \mu_1 = \mu_2$ and $H_{0,2} : \mu_1 = \mu_3$, and T_1 and T_2 are the standard t -statistics.

Suppose first that $H_{0,1}$ holds and $\mu_1 < \mu_3$. Then we expect $T_{1,0}$ to be close to zero, and $T_{2,0}$ to be large negative. On the other hand, if $T_{j,b}$, $j = 1, 2$ are computed from a permuted sample, then it is likely that $|T_{1,b}| > |T_{1,0}|$ and $T_{2,0} < T_{2,b}$.

Hence, the point $\mathbf{T}_0 = (T_{1,0}, T_{2,0})^\top$ is expected to be transported to a grid point close to $(0, -1)$. The corresponding vector of individual contributions would be $(0, 1)$ indicating that the two hypotheses contribute by 0 % and 100 % respectively. This situation is illustrated in an idealized example in the left upper panel of Figure 6. Here, the red point corresponds to the transported observed test statistic $F_{\pm}^{(B)}(\mathbf{T}_0)$ and it lies far from the centre in the direction of the violated marginal null hypothesis. As described previously, we reject the null hypothesis if $\|F_{\pm}^{(B)}(\mathbf{T}_0)\| > 1 - \alpha$. At the same time, the “downward” pointing arrow indicates that the rejection is due mainly to the second component of the composite null hypothesis.

Similar considerations hold also for the transportation of partial permutation p-values, which are, for this example, expected to be $p_1 \approx 1$ and p_2 small, leading to a complement vector \mathbf{q}_0 close to $(0, 1)$. Such point is then transported to $\tilde{F}_{\pm}^{(B)}(\mathbf{q}_0)$ close to $(0, 1)$, see the lower left panel of Figure 6. The red arrow again indicates how the individual tests contribute to the rejection of the null hypothesis.

Suppose now a different situation where $\mu_1 - \mu_3 = \gamma = -(\mu_1 - \mu_2)$ for some $\gamma > 0$, so the two marginal hypotheses contribute equally to the overall decision. The test statistic $T_{1,0}$ is expected to be large negative and $T_{2,0}$ to be large positive. An idealized example of a transport of such point \mathbf{T}_0 is provided in the upper right plot in Figure 6. Here, the direction \mathbf{D} of $F_{\pm}^{(B)}(\mathbf{T}_0)$ is $(-1/\sqrt{2}, 1/\sqrt{2})$, so the vector of individual contributions is $(1/2, 1/2)$. The vector of p-values for this example is expected to be close to $(0, 0)$, so the complement vector \mathbf{q}_0 is close to the extreme $(1, 1)$. This point is then transported to a grid point close to $(1/\sqrt{2}, 1/\sqrt{2})$.

In practice, the point \mathbf{T}_0 is not transported exactly as shown in the upper two panels of Figure 6 but $F_{\pm}^{(B)}(\mathbf{T}_0)$ is expected to be somewhere near the idealized point, depending on B and the chosen grid \mathcal{G}_B . The same holds for the transport of \mathbf{p}_0 . However, a simulation study presented in Section 5.2 reveals that the vector of individual contributions is on average very close to the true vector of contributions for both methods.

4.4. Modification for “mixed” alternatives. Recall that Section 4.1 assumed that all the partial problems are two-sided. Let \mathbf{T} be again a d -dimensional test statistic for testing H_0 . If all the partial tests are one-sided such that the corresponding hypothesis is rejected for large values, then the approach from Section 4.1 can be easily adapted to this situation by considering a grid \mathcal{G}_B^+ from Section 4.2.

More generally, assume that the partial tests reject for $|T_j|$ large (two-sided tests) for $j \in \mathcal{J} \subset \{1, \dots, d\}$, while other partial tests reject for T_j large (one-sided tests) for $j \in \{1, \dots, d\} \setminus \mathcal{J}$. The multivariate permutation test from Section 4.1 can be then adapted to this situation simply by considering a regular set of $B + 1$ points $\tilde{\mathcal{G}}_B$ in $\{\mathbf{x} : \|\mathbf{x}\| \leq 1, x_j \geq 0 \text{ for } j \in \{1, \dots, d\} \setminus \mathcal{J}\}$. Construction of such grid is essentially an analogue to the construction of \mathcal{G}_B and \mathcal{G}_B^+ .

4.5. Practical implementation. Let us discuss the steps 1., 2. and 4. of Algorithm 1 in more detail. A particular examples in R software (R Core Team, 2022) are provided online, on web page https://www.karlin.mff.cuni.cz/~hudecova/research/mult_perm/Main.html.

Step 1. It is common to take $B \approx 1000$ or larger in permutation tests. In our applications the choice of B is also related to the choice of the grid type, see Section 3.1. If one wishes to use a product form grid then it is suitable to chose B

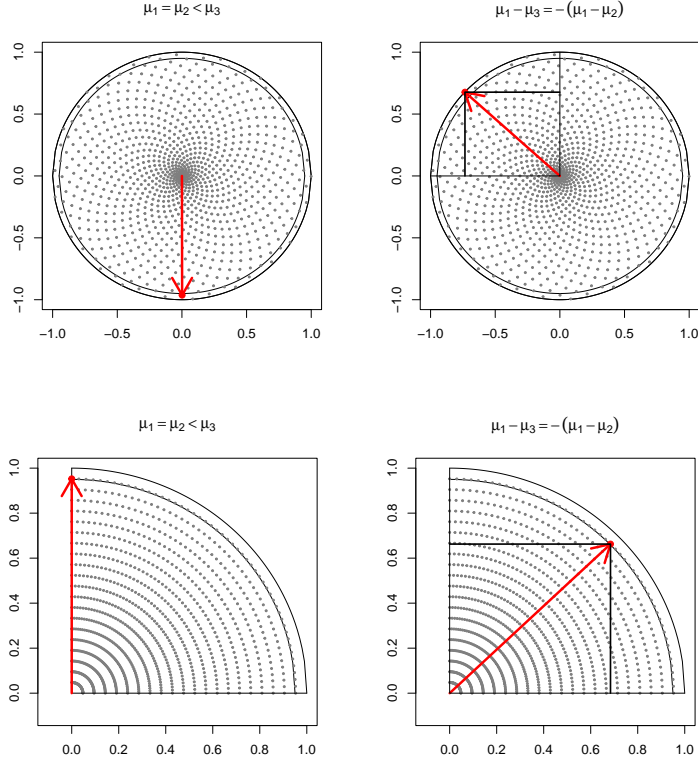


FIGURE 6. Decomposition of a significant test statistic in two setups, with $F_{\pm}^{(B)}(\mathbf{T}_0)$ denoted by a red arrow, into directions and partial contributions: as an illustration, two-sided test statistics and a non-product set \mathcal{N} are used in the first two plots (first row), partial permutation p-values and a product grid \mathcal{P}^+ are plotted in the second row.

such that $B + 1 = n_R n_S$ or $B + 1 = n_R n_S + 1$ (so n_0 is 0 and 1 respectively). The decomposition n_R and n_S should be chosen suitably with respect to the dimension d . Moreover, the smallest possible p-value \hat{p}_a is $1/(n_R + 1)$, so one has to take $n_R \geq 1/\alpha - 1$, where α is the chosen significance level. For $\alpha = 0.05$, this gives $n_R \geq 19$. Note that if $n_R \in [19, 38]$ then the null hypothesis is rejected only if $F_{\pm}^{(B)}(\mathbf{T}_0)$ lies on the most outer circle of the grid, i.e. $\|F_{\pm}^{(B)}(\mathbf{T}_0)\| = n_R/(n_R + 1)$.

If a non-product grid is going to be used there is no need for factorization into a product $n_R n_S$, but it is customary to take B such that $(B + 1) \cdot \alpha$ is an integer, where α is the chosen significance level. In that case we reject for if the value of \mathbf{T}_0 is transported to one of the $(B + 1) \cdot \alpha$ most extreme points of the grid (see also the online example). Moreover, if one wishes to use a GLP set to generate the $B + 1$ low-discrepancy points in $[0, 1]^d$ then B should be chosen with respect to this fact, because there are some practical limitations, see below.

Step 2. For $d > 2$ both types of grids require a construction of a low-discrepancy sequence in $[0, 1]^r$ for either $r = d - 1$ or $r = d$. As mentioned in Section 3.1, this sequence can be obtained by either a Halton method or a Sobor method, which are both available in R in package `randtoolbox` (Dutang and Savicky, 2022). As an alternative construction, used also in some examples in this paper, one can compute the so-called good lattice point (GLP) set described in Fang and Wang (1994, Section 1.3), where the lattice points set of size $B + 1$ in $[0, 1]^d$ is obtained by calculating a set of properly rescaled modulo $(B + 1)$ multiples of a selected generating vector $h = (h_1, \dots, h_d)^\top$. It can be shown that, for certain values of B , appropriately chosen generating vector leads to a well uniformly scattered set of points (Korobov, 1959; Hlawka, 1962). A table of optimal generating vectors for various B and d is given, e.g., in Fang and Wang (1994, Appendix A). This means that a GLP sequence of length $B + 1$ with low discrepancy in $[0, 1]^d$ can be easily generated only for some particular values of $B + 1$. However, this should not be seen as a serious restriction because the number of permutations B can be chosen quite flexibly.

Step 4. For a given grid set \mathcal{G}_B the transportation $F_{\pm}^{(B)}$ can be computed using so called Hungarian algorithm (Papadimitriou and Steiglitz, 1982) which is implemented for instance in package `clue` in R.

5. SIMULATION STUDY

Let us now investigate the concept in a small simulation study. We start with a simple example, similar to the simulated example from Section 2.1.

5.1. Testing for means under homoscedasticity. Consider a homoskedastic three sample problem, where we generate independent observations $X_{j,i} \sim N(\mu_j, \sigma^2)$, $i = 1, \dots, n_j$ for samples $j \in \{1, 2, 3\}$ and for $n_1 = n_2 = n_3$.

Our three basic simulation setups are as follows:

$$\begin{aligned} H_0: & \mu_1 = \mu_2 = \mu_3 = 0, \\ A_\delta: & \mu_1 = \mu_2 = 0, \mu_3 = \delta, \\ B_\delta: & \mu_1 = 0, \mu_2 = \delta/2 = -\mu_3, \end{aligned}$$

with the parameter $\delta \in \{1, 2\}$, $\sigma^2 = 1$, $n_1 \in \{5, 10\}$.

In this setup, it can be expected that very good results will be achieved by the usual F-test. Following the example from Section 2, the F-test will be compared to the multivariate permutation test (Algorithm 1) based on the optimal transportation of the bivariate t-test statistic $\mathbf{T} = (T_1, T_2)^\top$, where T_1 compares the first and the second sample and T_2 compares the first and the third sample. Next to this, we also compute the optimal transport and the corresponding p-value of the one-sided test statistic $\tilde{\mathbf{T}} = (|T_1|, |T_2|)^\top$, and the transport of the vector of partial permutation p-values (Algorithm 2). The result are compared to the classical multivariate permutation tests utilizing the most commonly used Tippett, Fisher, and Liptak combining functions described in Section 2. More precisely, we compare the following tests:

- F : usual F-test (based on F quantiles),
- $c(T)$: multivariate permutation test with the Tippett combining function,
- $c(F)$: multivariate permutation test with the Fisher combining function,
- $c(L)$: multivariate permutation test with the Liptak combining function,
- $t(\mathcal{P})$: transport of the two-sided test statistic \mathbf{T} to a product grid \mathcal{P} ,

	n_1	F	$c(T)$	$c(F)$	$c(L)$	$t(\mathcal{P})$	$t(\mathcal{N})$	$t(\mathcal{P}^+)$	$t(\mathcal{N}^+)$	$p(\mathcal{P}^+)$	$p(\mathcal{N}^+)$
H_0	5	4.1	4.4	5.3	5.7	3.5	4.8	5.0	5.6	4.9	5.4
	10	6.4	4.9	5.1	4.1	4.8	4.4	5.2	5.7	6.1	4.7
A_1	5	25.5	22.6	16.0	14.4	24.4	24.2	18.6	19.7	20.4	19.2
	10	57.1	48.8	35.6	19.5	52.5	47.9	45.9	46.2	43.4	45.3
A_2	5	84.2	67.0	50.8	33.8	72.3	72.5	63.7	65.7	68.3	63.5
	10	99.4	97.4	94.4	60.6	99.1	98.1	97.0	97.4	96.2	94.5
B_1	5	24.5	13.2	7.5	7.0	20.6	22.5	10.5	11.1	13.1	11.3
	10	45.1	24.8	19.3	11.2	43.0	44.0	20.2	20.7	22.6	23.1
B_2	5	70.2	36.3	31.8	31.5	65.1	64.1	34.6	34.5	34.5	34.2
	10	97.1	76.0	79.6	76.1	95.4	95.2	76.3	76.6	70.5	70.0

TABLE 1. Empirical size and power (in %) of multivariate permutation tests using combining functions and optimal transport in a three sample testing problem, sample sizes $n_1 = n_2 = n_3$, $n_1 \in \{5, 10\}$, homoskedastic case with $\sigma^2 = 1$, significance level $\alpha = 0.05$, 1000 simulations, bold font denotes two most powerful permutation tests in each simulation setup.

$t(\mathcal{N})$: transport of the two-sided test statistics \mathbf{T} to a non-product grid \mathcal{N} ,
 $t(\mathcal{P}^+)$: transport of the one-sided test statistics $\tilde{\mathbf{T}}$ to the positive product grid \mathcal{P}^+ ,
 $t(\mathcal{N}^+)$: transport of the one-sided test statistics $\tilde{\mathbf{T}}$ to the positive non-product grid \mathcal{N}^+ ,
 $p(\mathcal{P}^+)$: transport of the vector of partial permutation p-values to \mathcal{P}^+ ,
 $p(\mathcal{N}^+)$: transport of the vector of partial permutation p-values to \mathcal{N}^+ .

For all variants of the multivariate permutation test, we use $B = 999$ permutations with the exception of the non-product grid, because its construction is based on a GLP set of $B + 1$ points, and it is described in Section 4.5 that only some specific choices of $B + 1$ are possible in this case. Hence, for a non-product grid we set $B + 1 = 987$ and the GLP sequence in $[0, 1]^2$ is computed using generating vector $h = (1, 610)^\top$, as recommended in Fang and Wang (1994, Appendix A). The product form grid was generated with $n_0 = 0$, $n_R = 20$, and $n_S = 50$ for the two-sided test statistic and $n_R = 40$ and $n_S = 25$ for the one-sided tests. In the two-sided setup, the null hypothesis is rejected on level $\alpha = 0.05$ if and only if the transported test statistics falls in the outermost ring (with p-value equal to $1/21 \doteq 0.0476$). In the one-sided setup, the null hypothesis is rejected on level $\alpha = 0.05$ if the test statistic falls in the two outermost rings, i.e., for p-value $1/41$ or $2/41$.

Simulation results are summarized in Table 1. For all tests, the empirical level is reasonably close to the nominal level $\alpha = 0.05$. Looking at the simulation setup A_δ , the highest power is always achieved by the F-test, followed closely by the optimal transport permutation tests using the two-sided test statistics. Somewhat smaller power is obtained by looking at the univariate test statistics or the p-values (using either the Fisher combining function or the optimal transport approach). Interestingly, the advantages of using the two-sided test statistics are even clearer in the simulation setup B_δ , where the largest difference (between groups 2 and 3) is not considered directly in the test statistics T_1 and T_2 .

	$t(\mathcal{P})$		$t(\mathcal{N})$		$t(\mathcal{P}^+)$		$t(\mathcal{N}^+)$		$p(\mathcal{P}^+)$		$p(\mathcal{N}^+)$	
A_1	95%	1.57π	94%	1.58π	91%	0.40π	91%	0.40π	88%	0.39π	88%	0.39π
A_2	98%	1.55π	98%	1.54π	98%	0.46π	98%	0.45π	93%	0.41π	93%	0.41π
B_1	49%	0.75π	49%	0.75π	50%	0.25π	51%	0.25π	51%	0.25π	50%	0.25π
B_2	50%	0.75π	49%	0.75π	49%	0.25π	51%	0.25π	48%	0.24π	50%	0.25π

TABLE 2. Percentage contribution of the second hypothesis and angles φ of $F_{\pm}^{(n)}(\mathbf{T}_0)$. The averages are computed over significant simulation results, significance level $\alpha = 0.05$, $n_1 = 10$ observations in each sample.

5.2. Decomposition to partial contributions. As described in Section 4.3, the optimal transport approach provides additional information on the importance of the marginal hypotheses, which is a crucial difference compared to the F-test or the multivariate permutation tests. For $d = 2$ the vector of individual contributions is (D_1^2, D_2^2) , so it suffices to look at one component of this vector. Alternatively, one can look at the angle between the x axis and the vector (D_1, D_2) , i.e. φ such that $D_1 = \cos \varphi$ and $D_2 = \sin \varphi$.

In order to elucidate this concept, the simulated average angles φ and partial contributions $D_2^2 \cdot 100\%$ (percentage contribution of T_2) are reported in Table 2. Recall that T_1 tests $H_{0,1} : \mu_1 = \mu_2$, while T_2 corresponds to $H_{0,2} : \mu_1 = \mu_3$. In A_δ setup $H_{0,1}$ holds, so only T_2 should contribute to the rejection, and the idealized value of (D_1, D_2) is $(0, 1)$ corresponding to $\varphi = 3\pi/2$ and $D_2^2 = 1$, see also the top left panel of Figure 6. This is confirmed in Table 2 by values in columns corresponding to $t(W)$ and $t(G)$. If the absolute values $|T_j|$, $j = 1, 2$, are considered, then (D_1, D_2) is expected to be close to $(0, 1)$, corresponding to the angle $\pi/2$. The empirical counterparts in columns $t(\mathcal{P}^+)$, $t(\mathcal{N}^+)$ seem to be slightly further from the expected quantities, and the same conclusion is obtained for the transport of the multivariate p-values, reported in columns $p(\mathcal{P}^+)$ and $p(\mathcal{N}^+)$, where the agreement with the expected quantities seems to be the worst. Also, the larger δ , the closer the empirical quantities are to the nominal ones.

The setting B_δ corresponds to the idealized situation plotted in the two right panels of Figure 6. So for the transport of $(T_1, T_2)^\top$, $(|T_1|, |T_2|)^\top$ and $(p_1, p_2)^\top$ the expected angles are $3\pi/4$, $\pi/2$ and $\pi/2$ respectively, and the contribution of T_2 is expected to be 50%. The sample analogous in Table 2 are very close to these nominal values for all three cases. Here the difference between results for $\delta = 1$ and $\delta = 2$ is negligible.

To sum up, the results under both alternatives confirm that the direction \mathbf{D} of the transported observed test statistic $F_{\pm}^{(n)}(\mathbf{T}_0)$ really may be used as a tool for uncovering the underlying reasons for rejecting the composite null hypothesis.

5.3. Testing for means under heteroscedasticity. The effect of heteroscedasticity is shortly investigated in a simulation summarized in Table 3. The setup remains exactly the same as in Table 1, but the standard deviation in the third group is set to $\sigma_3 = 4$. It is important to note that in this setup, with different standard deviations, the data are not exchangeable even if $\mu_1 = \mu_2 = \mu_3$. Hence, the permutation test is actually testing the null hypothesis of ‘equality in distribution’ even though the test statistics are based on sample mean differences. Thus,

	n_1	F	$c(T)$	$c(F)$	$c(L)$	$t(\mathcal{P})$	$t(\mathcal{N})$	$t(\mathcal{P}^+)$	$t(\mathcal{N}^+)$	$p(\mathcal{P}^+)$	$p(\mathcal{N}^+)$
H_0	5	10.1	7.5	7.7	5.6	11.8	11.7	10.9	9.0	9.9	8.5
	10	9.5	7.6	6.6	5.2	8.0	9.2	7.8	6.6	7.8	7.6
A_1	5	14.2	14.3	10.5	6.0	14.4	17.0	12.4	10.8	13.0	13.7
	10	18.0	11.7	9.3	8.1	16.8	16.9	13.4	14.1	13.7	12.9
A_2	5	23.5	22.7	18.6	12.2	21.7	23.8	20.6	20.9	21.1	22.1
	10	39.8	29.5	25.8	16.4	33.2	33.2	29.0	28.3	26.6	26.4
B_1	5	12.0	13.7	14.7	7.4	20.6	20.2	13.3	15.1	16.6	13.5
	10	14.8	20.2	14.9	12.3	26.2	27.7	16.4	15.8	19.9	17.6
B_2	5	20.9	30.0	26.6	20.2	40.4	40.1	32.5	30.7	30.5	33.2
	10	31.4	52.5	51.1	35.1	66.1	69.3	51.3	52.9	51.6	52.2

TABLE 3. Empirical power (in %) for the F-test and multivariate permutation tests in a heteroskedastic three-sample setup ($\sigma_1 = \sigma_2 = 1$, $\sigma_3 = 4$), bold font denotes the two most powerful permutation tests in each simulation setup.

	$(\mu_1, \mu_2, \mu_3, \mu_4)$	F	$c(T)$	$c(F)$	$c(L)$	$t(\mathcal{P})$	$t(\mathcal{N})$	$t(\mathcal{P}^+)$	$t(\mathcal{N}^+)$	$p(\mathcal{P}^+)$	$p(\mathcal{N}^+)$
N	(0, 0, 0, 0)	4.3	5.0	5.2	5.6	4.4	5.2	5.0	4.0	4.9	4.6
	(0, 0, 3, 1)	51.0	56.8	41.6	32.2	45.5	35.4	48.7	42.6	37.4	30.4
	(0, 0.5, 2, 1)	20.7	19.4	20.4	17.0	16.9	13.1	19.0	19.0	17.4	15.1
	(0, 1, 2, 3)	42.8	38.9	45.1	41.0	36.5	27.1	42.1	38.1	36.7	33.5
	(0, 2, -1, 3)	78.0	65.2	75.4	73.5	67.4	49.6	71.4	68.3	62.1	57.6
	(1, 3, 0, 2)	45.7	37.2	46.1	39.8	39.1	33.2	44.6	39.4	36.1	30.7
χ^2	(0, 0, 0, 0)	4.1	4.0	4.7	4.3	4.6	4.3	5.1	4.9	4.6	5.3
	(0, 0, 3, 1)	58.2	63.5	54.4	32.4	52.8	44.8	55.5	52.2	40.9	31.2
	(0, 0.5, 2, 1)	24.7	29.5	27.3	17.9	24.3	19.8	27.4	23.2	18.6	19.4
	(0, 1, 2, 3)	51.9	43.7	50.6	48.2	52.9	33.5	49.2	47.4	41.7	41.0
	(0, 2, -1, 3)	77.7	66.8	79.7	77.1	75.5	47.0	78.0	74.4	66.3	63.5
	(1, 3, 0, 2)	51.0	45.1	53.9	48.2	50.5	39.5	49.6	45.0	44.9	40.9

TABLE 4. Empirical power (in %) in a four-sample problem, six scenarios, symmetric (centered Normal distribution) or skewed random errors (centered χ_2^2 distribution) with variance 4, Helmert contrasts, $n_i = 5$, $i \in \{1, \dots, 4\}$, bold font denotes two most powerful permutation tests in each simulation setup.

the rows denoted as H_0 in Table 3 simply correspond to the setup where we take $\mu_1 = \mu_2 = \mu_3$ and one should not be surprised that the corresponding proportions of rejections exceed the nominal level 5%.

Similarly as in the homoskedastic setup, the empirical power reported in Table 3 is highest for the test based on optimal transport of the two-sided test statistics, followed by the remaining versions of the permutation test. Interestingly, the F-test actually performs quite poorly especially in the simulation setup B_δ .

5.4. Four sample comparisons with Helmert contrasts. Let us now consider a four sample problem, where $X_{j,i} = \mu_j + \varepsilon_{j,i}$, $j = 1, \dots, 4$, $i = 1, \dots, n_j$ for

$(\mu_1, \mu_2, \mu_3, \mu_4)$	$t(\mathcal{P})$	$t(\mathcal{N})$	$t(\mathcal{P}^+)$	$t(\mathcal{N}^+)$	$p(\mathcal{P}^+)$	$p(\mathcal{N}^+)$
(0, 0, 3, 1)	0/100/0	0/100/0	8/84/8	8/84/8	11/79/10	10/80/10
(0, 0.5, 2, 1)	5/93/2	6/93/1	18/65/17	19/64/16	19/63/18	20/64/15
(0, 1, 2, 3)	10/32/58	9/29/62	15/31/54	15/32/53	17/32/51	19/29/52
(0, 2, -1, 3)	20/27/53	20/30/51	20/25/55	21/28/51	25/29/46	23/30/47
(1, 3, 0, 2)	43/51/6	39/53/8	39/48/13	38/48/14	37/47/16	38/47/15

TABLE 5. Importance of marginal hypotheses (in %) in a four-sample problem, five scenarios, Helmert contrasts, Normal distribution, $\sigma = 2$, $n_i = 5$, $i \in \{1, \dots, 4\}$.

$n_1 = n_2 = n_3 = n_4$, with independent random errors generated either from a symmetric (centered normal distribution with variance $\sigma^2 = 4$) or skewed distribution (centered χ^2 distribution with 2 degrees of freedom) with the same variance. The null hypothesis

$$H_0 : \mu_1 = \mu_2 = \mu_3 = \mu_4$$

will be tested using Helmert contrasts, that is via partial null hypotheses

$$H_{0,1} : \mu_2 - \mu_1 = 0, \quad H_{0,2} : \mu_3 - \frac{\mu_2 + \mu_1}{2} = 0, \quad H_{0,3} : \mu_4 - \frac{\mu_1 + \mu_2 + \mu_3}{3} = 0.$$

The corresponding test statistic \mathbf{T} is three dimensional and its components are the t-tests statistics corresponding to the three contrasts. Again, the F-test of H_0 (based on F quantiles) serves as a baseline and it is compared to the various approaches to multivariate permutation tests.

The simulation results summarized in Table 4 show that the highest power is achieved either by the multivariate permutation tests with combining functions or by the multivariate permutation test using optimal transport of the partial permutation p-values to the positive part of the three-dimensional product form grid; note also that the optimal transport to the product form grid consistently outperforms the optimal transport to the three-dimensional non-product grid.

This could be partly explained by an insufficient grid size $B+1$, and it is expected that the difference in results for the two types of grids will vanish with increasing B . Recalculating the power for a two-sided test statistic with a non-product type grid in the last row of Table 4 using 200 simulations and a grid of size $B+1 = 8190$ leads to an empirical power 59 % (instead of 39 %), clearly outperforming all other tests in the same setup. Unfortunately, increasing the grid size is very computationally expensive.

It is also interesting to note that the power of all tests in Table 4 is larger for the skewed random errors compared to the normal errors. This is, however, in agreement with some previous findings, see, e.g., Tiku (1971).

Table 5 summarizes the averaged partial contributions $(D_1^2, D_2^2, D_3^2) \cdot 100\%$ of the three underlying null hypothesis. Similarly as in Table 2, it seems that the optimal transport approach allows to identify correctly the relative importance of the underlying marginal hypotheses.

5.5. Two-sample comparisons of mean and variance. For the last Monte Carlo simulation consider a two sample problem, where observations from the j -th sample, $j \in \{1, 2\}$, are generated as $X_{j,i} = \mu_j + \sigma_j \varepsilon_{j,i}$, $i = 1, \dots, n$, where the independent random errors $\varepsilon_{j,i}$ have either symmetric (standard normal) or skewed

	μ_2	σ_2	T_{12}	F_{12}	$c(T)$	$c(F)$	$c(L)$	$t(\mathcal{P})$	$t(\mathcal{N})$	$t(\mathcal{P}^+)$	$t(\mathcal{N}^+)$	$p(\mathcal{P}^+)$	$p(\mathcal{N}^+)$
N	0	2	5.3	5.4	5.5	5.9	5.4	5.3	4.6	4.8	4.6	5.5	5.8
	2	2	59.1	6.3	45.3	43.1	35.4	39.6	35.8	40.8	43.6	41.5	43.3
	0	4	3.9	48.7	30.2	32.7	23.6	25.9	23.4	29.8	28.6	25.9	26.9
	2	4	26.1	47.3	43.3	50.8	49.8	40.8	34.1	47.6	49.4	42.9	47.3
χ_2^2	0	2	4.9	23.0	5.1	4.5	5.2	5.1	4.5	4.6	5.1	5.0	5.7
	2	2	60.9	23.4	62.9	52.4	39.9	77.7	73.9	62.7	57.7	64.2	60.0
	0	4	7.5	50.1	29.4	22.6	15.8	39.4	39.8	30.2	29.8	32.7	32.0
	2	4	24.2	52.1	24.9	25.4	24.5	17.1	15.2	20.5	21.7	22.5	21.2

TABLE 6. Empirical level and power (in %) in a two-sample problem combining the tests of equality of expectations (T_{12} , two-sample t-test) and variances (F_{12} , F test for equality of variance), $\mu_1 = 0$, $\mu_2 \in \{0, 2\}$, $\sigma_1 = 2$, $\sigma_2 \in \{2, 4\}$, $n_1 = n_2 = 10$, level $\alpha = 0.05$, 1000 simulations, standard normal or standardized χ_2^2 random errors, bold font denotes two most powerful permutation tests in each simulation setup.

(centered and standardized χ_2^2 distribution). In both simulation setups $EX_{j,i} = \mu_j$ and $\text{Var}X_{j,i} = \sigma_j^2$ and we are interested in testing the composite null hypothesis $H_0 : \mu_1 = \mu_2 \ \& \ \sigma_1^2 = \sigma_2^2$ against general alternatives. This is a special case of the problem described in Section 2.2.1 for $K = 2$ samples and $r = 2$ moments.

Obviously, the means can be compared using a two-sample t-test statistic, say T_{12} , and the ratio of sample variances $F_{12} = S_1^2/S_2^2$ can be used for testing equality of variances. Apart of performing these two tests separately, using the critical values based on t - and F -distribution, we apply also the multivariate permutation tests utilizing the bivariate test statistic $(T_{12}, \log(F_{12}))^\top$, where $\log(F_{12})$ is used mainly in order to facilitate the calculations for the two- and one-sided tests used in the optimal transport approach.

Table 6 reports the percentage of rejection of H_0 for several tests under various alternatives. For normally distributed random errors, all tests behave as expected, with overall best behaviour observed for the Fisher combining function. Looking at the optimal transport-based tests, the power seems to be more stable (with respect to the grid choice) and only slightly smaller than the power achieved by the best combining function.

In the second part of Table 6, corresponding to non-symmetrically distributed random errors, one can observe a slightly larger power of the two-sample t-test and a complete failure of the variance equality F-test (with an empirical level equal to 23%) that is in agreement with its well-known non-robustness (Lehmann and Romano, 2005, Section 11.3). Concerning the permutation tests, two-sided test statistics clearly outperform all other tests if only one of the marginal hypotheses does not hold. One-sided approaches using either the one-sided test statistics or p-values lead similar results in most setups. Hence, one can conclude that the optimal transport approach seems to be more stable, with slightly better performance in setups with only one violated marginal hypothesis.

The percentages of contributions of partial tests are summarized in Table 7. The results for the normal distribution seem to be more readable, with the percentages quite clearly identifying the correct alternatives, especially in the two-sided

	μ_2	σ_2	$t(\mathcal{P})$	$t(\mathcal{N})$	$t(\mathcal{P}^+)$	$t(\mathcal{N}^+)$	$p(\mathcal{P}^+)$	$p(\mathcal{N}^+)$
N	2	2	100/0	100/0	89/11	88/12	86/14	85/15
	0	4	0/100	0/100	16/84	17/83	18/82	19/81
	2	4	38/62	40/60	42/58	43/57	39/61	41/59
χ_2^2	2	2	88/12	90/10	91/9	89/11	85/15	84/16
	0	4	20/80	18/82	19/81	17/83	17/83	19/81
	2	4	78/22	77/23	66/34	65/35	63/37	62/38

TABLE 7. Importance of partial tests (in %) in a two-sample problem combining the tests of equality of expectations and variances.

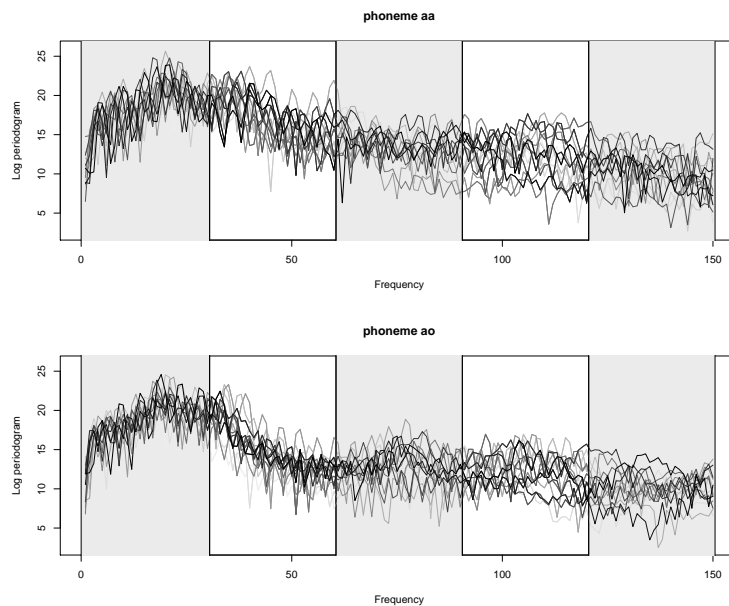


FIGURE 7. Log periodograms for phonemes “aa” and “ao”, $n_1 = n_2 = 15$, with frequencies split to five segments, source: R library `fds` (Shang and Hyndman, 2018).

approach. For skewed random errors, the empirical contributions seem to be a bit more “fuzzy” but, in all cases, the percentages corresponding to valid null hypotheses are smaller than 20% whereas the percentages corresponding to valid alternatives are always greater than 80%.

6. APPLICATION TO FUNCTIONAL DATA

Hlávka et al. (2022) investigated the phoneme data set plotted in Figure 7 and observed statistically significant differences in the distribution of the two functional random samples (using a test comparing empirical characteristic functions) in the first three of five segments (with sample size 15 in each sample). These results were confirmed by applying separate permutation tests of equality of mean functions (test statistic F_{\max}) (Górecki and Smaga, 2019) and covariance operators (test

	1.	2.	3.	4.	5.
mean (Fmax)	0.443	0.002	0.001	0.828	0.708
covariance (SQ)	0.039	0.005	0.075	0.505	0.123
Tippett	0.071	0.003	0.001	0.752	0.227
Fisher	0.113	0.001	0.001	0.775	0.287
Liptak	0.138	0.001	0.001	0.751	0.329
$t(\mathcal{P}^+)$	0.048 (8%)	0.048 (95%)	0.048 (100%)	0.762	0.286
$t(\mathcal{N}^+)$	0.081 (4%)	0.011 (92%)	0.001 (100%)	0.797	0.274
$p(\mathcal{P}^+)$	0.095 (4%)	0.048 (52%)	0.048 (61%)	0.762	0.286
$p(\mathcal{N}^+)$	0.059 (6%)	0.018 (51%)	0.013 (63%)	0.762	0.295

TABLE 8. P-values of permutation tests for equality of mean functions (Fmax) and covariance operators (SQ) in five segments of the phoneme data set together with p-values obtained by nonparametric combination and optimal transport, $n_1 = n_2 = 15$, importance of the first marginal hypothesis (in %) is calculated for optimal transport based permutation tests.

statistic SQ based on square-root distance) (Cabassi et al., 2017) reported in the first two rows in Table 8.

As described in Section 2.2.2, the joint null hypothesis of equality of the mean functions and the covariance operator can be tested using the multivariate permutation test. In Table 8, we report the p-values obtained by nonparametric combination (Tippett, Fisher, and Liptak combining functions) and also p-values obtained by the optimal transport of the one-sided test statistic or partial permutation p-values. In segment 1, the composite null hypothesis is rejected only using the optimal transport approach of the test statistic on the product form grid \mathcal{P}^+ although p-values obtained by other approaches are also quite close to 0.05. The percentages (8%/92%) indicate that the significant difference between the two samples in the first segment is caused mostly by the violation of the second null hypothesis and the reason for rejecting the composite null hypothesis in the first segment is a different covariance structure.

In the remaining segments, all multivariate permutation tests arrive to the same conclusions. The p-value based on the product form grid sometimes seems to be somewhat larger but $0.048 \doteq 1/21$ is actually the smallest possible p-value (corresponding to the outermost ring in the product form grid). The partial contributions obtained for one-sided test statistic suggest that the differences in mean functions are more responsible for rejecting the null hypothesis in segments 2 and 3. Interestingly, the partial contributions obtained for the p-values seem to have a different interpretation since, in this case, both partial p-values are quite small and, in this sense, i.e., from a point of view of the partial p-values, both marginal null hypotheses contribute almost equally to the rejection of the composite null hypothesis.

7. SUMMARY

This paper proposes to combine the optimal transport methods with multivariate permutation tests. It is shown that the empirical transport of a multivariate permutation test statistics leads to a well-defined single p-value, which can be also

interpreted as a measure of conformity of the observed multivariate test statistic with the (simulated) permutation sample.

In contrast to the classical approach to multivariate permutation tests utilizing the so-called nonparametric combination, the proposed method allows to evaluate also the contributions of the partial test statistics to the rejection of the null hypothesis, providing additional insights. The definition of absolute contributions guarantees that the null hypothesis is rejected if and only if the sum of these absolute contributions is larger than the desired confidence level. For a large number of comparisons, these relative contributions could be presented in a suitable graph, similar to the scree plot of eigenvalues in principal component analysis, summarizing the influence of partial test statistics and indicating main reasons for rejecting the composite null hypothesis.

The Monte Carlo simulation study reveals that, in some setups, the optimal transport approach to multivariate permutation tests clearly outperforms the classical nonparametric combination. This holds especially in setups, in which the transformation to p-values (or one-sided test statistics) leads to some loss of information (see Table 3), with skewed random errors, or when some of the marginal null hypotheses hold true (see Table 6). In other situations, nonparametric combination with properly chosen combining function performs very well but, unfortunately, the best combining function usually cannot be reliably chosen in advance unless we have some prior information concerning the alternative. Therefore, in general, it may be safer to use the optimal transport approach, circumventing the possibility of choosing the combining function inappropriately.

In a simulation study, we have compared two asymptotically equivalent grids that typically lead comparable results in lower-dimensional problems, although the behavior of the product-type grid seems to be a bit more stable. The simulation study also suggests that the number of points should be larger for two-sided test statistics and for the non-product type grid. Theoretically, the proposed approach is directly applicable for an arbitrary number of comparisons but, since the grid size should increase exponentially with the dimension, the necessary calculations may soon become computationally unfeasible. Speeding up these calculations thus remains a challenging future research problem that may make the optimal transport approach applicable even with large number of simultaneous comparisons.

REFERENCES

- Bugni, F. A. and Horowitz, J. L. (2021). Permutation tests for equality of distributions of functional data. *J. Appl. Econometrics*, 36(7):861–877.
- Cabassi, A., Pigoli, D., Secchi, P., and Carter, P. A. (2017). Permutation tests for the equality of covariance operators of functional data with applications to evolutionary biology. *Electron. J. Stat.*, 11(2):3815–3840.
- Cardot, H., Prchal, L., and Sarda, P. (2007). No effect and lack-of-fit permutation tests for functional regression. *Comput. Statist.*, 22:371–390.
- Chandler, G. and Polonik, W. (2022). Antimodes and graphical anomaly exploration via depth quantile functions. arXiv:2201.06682.
- Chaudhuri, P. (1996). On a geometric notion of quantiles for multivariate data. *J. Amer. Statist. Assoc.*, 91:862–872.
- Chernozhukov, V., Galichon, A., Hallin, M., and Henry, M. (2017). Monge-Kantorovich depth, quantiles, ranks and signs. *Ann. Statist.*, 45(1):223–256.

- Cuesta-Albertos, J. A. and Febrero-Bande, M. (2010). A simple multiway ANOVA for functional data. *TEST*, 19(3):537–557.
- Cuevas, A., Febrero, M., and Fraiman, R. (2004). An ANOVA test for functional data. *Comput. Statist. Data Anal.*, 47(1):111–122.
- Dutang, C. and Savicky, P. (2022). *randtoolbox: Generating and Testing Random Numbers*. R package version 2.0.3.
- Fang, K. and Wang, Y. (1994). *Number-theoretic Methods in Statistics*. Chapman & Hall.
- Figalli, A. and Glaudo, F. (2021). *An Invitation to Optimal Transport, Wasserstein Distances, and Gradient Flows*. EMS Press.
- Ghosal, P. and Sen, B. (2022). Multivariate ranks and quantiles using optimal transport: Consistency, rates and nonparametric testing. *Ann. Statist.*, 50(2):1012–1037.
- Górecki, T. and Smaga, L. (2015). A comparison of tests for the one-way ANOVA problem for functional data. *Comput. Statist.*, 30(4):987–1010.
- Górecki, T. and Smaga, L. (2019). *fdANOVA*: an R software package for analysis of variance for univariate and multivariate functional data. *Comput. Statist.*, 34(2):571–597.
- Hallin, M., del Barrio, E., Cuesta-Albertos, J., and Matrán, C. (2021). Distribution and quantile functions, ranks and signs in dimension d : A measure transportation approach. *Ann. Statist.*, 49(2):1139 – 1165.
- Hallin, M., Hlubinka, D., and Hudecová, Š. (2022). Efficient fully distribution-free center-outward rank tests for multiple-output regression and manova. *J. Amer. Statist. Assoc.* doi 10.1080/01621459.2021.2021921.
- Hallin, M., La Vecchia, D., and Liu, H. (2023). Rank-based testing for semiparametric VAR models: A measure transportation approach. *Bernoulli*, 29(1):229–273.
- Hallin, M. and Mordant, G. (2023). On the finite-sample performance of measure-transportation-based multivariate rank tests. In Yi, M. and Nordhausen, K., editors, *Robust and Multivariate Statistical Methods: Festschrift in Honor of David E. Tyler*, pages 87–119. Springer International Publishing.
- Halton, J. H. (1960). On the efficiency of certain quasi-random sequences of points in evaluating multi-dimensional integrals. *Numer. Math.*, 2:84–90.
- Hlávka, Z., Hlubinka, D., and Koňasová, K. (2022). Functional ANOVA based on empirical characteristic functionals. *J. Multivariate Anal.*, 189:104878.
- Hlawka, E. (1962). Zur angenäherten berechnung mehrfacher integrale. *Monatsh. Math.*, 66(2):140–151.
- Hlubinka, D. and Hudecová, Š. (2023). One sample location test based on the center-outward signs and ranks. *submitted*.
- Hlubinka, D., Kotík, L., and Šíman, M. (2022). Multivariate quantiles with both overall and directional probability interpretation. *Scand. J. Stat.*, 49:1586 – 1604.
- Hlubinka, D. and Šíman, M. (2015). On generalized elliptical quantiles in the nonlinear quantile regression setup. *TEST*, 24:249–264.
- Kashlak, A. B., Myroshnychenko, S., and Spektor, S. (2023). Analytic permutation testing for functional data anova. *J. Comput. Graph. Statist.*, 32(1):294–303.
- Korobov, N. (1959). Computation of multiple integrals by the method of optimal coefficients. *Vestnik Moskov. Univ. Ser. Mat. Meh. Astr. Fiz. Him*, 4:19–25.
- Koshevoy, G. A. and Mosler, K. (1998). Lift zonoids, random convex hulls and the variability of random vectors. *Bernoulli*, 4:377–399.

- Kost, J. T. and McDermott, M. P. (2002). Combining dependent p-values. *Statist. Probab. Lett.*, 60:183–190.
- Lehmann, E. L. and Romano, J. (2005). *Testing Statistical Hypotheses*. Springer-Verlag, New York, 3rd edition.
- Liu, D., Liu, R. Y., and Xie, M. (2022). Nonparametric fusion learning for multiparameters: Synthesize inferences from diverse sources using data depth and confidence distribution. *J. Amer. Statist. Assoc.*, 117(540):2086–2104.
- McCann, R. J. (1995). Existence and uniqueness of monotone measure-preserving maps. *Duke Math. J.*, 80:309–323.
- Papadimitriou, C. and Steiglitz, K. (1982). *Combinatorial Optimization: Algorithms and Complexity*. Prentice Hall.
- Pesarin, F. (2001). *Multivariate permutation tests: with applications in biostatistics*. Wiley.
- Pokorný, D., Laketa, P., and Nagy, S. (2023). Another look at half-space depth: Flag halfspaces with applications. *J. Nonparametr. Stat.* <https://doi.org/10.1080/10485252.2023.2236721>.
- R Core Team (2022). *R: A Language and Environment for Statistical Computing*. R Foundation for Statistical Computing, Vienna, Austria.
- Shang, H. L. and Hyndman, R. J. (2018). *fds: Functional Data Sets*. R package version 1.8.
- Shi, B. and Ogden, R. T. (2021). Inference in functional mixed regression models with applications to positron emission tomography imaging data. *Stat. Med.*, 40(21):4640–4659.
- Shi, H., Hallin, M., Drton, M., and Han, F. (2022). On universally consistent and fully distribution-free rank tests of vector independence. *Ann. Statist.*, 50(4):1933–1959.
- Sobol, I. (1967). The distribution of points in a cube and the approximate evaluation of integrals. *U.S.S.R. Comput. Math. and Math. Phys.*, 7:86–112.
- Tiku, M. L. (1971). Power function of the F-test under non-normal situations. *J. Amer. Statist. Assoc.*, 66(336):913–916.
- Villani, C. (2021). *Topics in optimal transportation*, volume 58. American Mathematical Soc.
- Vovk, V. and Wang, R. (2020). Combining p-values via averaging. *Biometrika*, 107(4):791—808.
- Zhang, H. and Wu, Z. (2023). The generalized Fisher’s combination and accurate p-value calculation under dependence. *Biometrics*, 79(2):533–1590.
- Zhang, J.-T. (2013). *Analysis of Variance for Functional Data*. CRC Press, New York.